NUMERICAL EVALUATION OF GEOMETRIC IMPEDANCE FOR SOLEIL

R. Nagaoka, Synchrotron SOLEIL, Gif-sur-Yvette, France

Abstract

The geometric impedance of the SOLEIL ring is pursued by numerically evaluating difference vacuum chamber components. Some of the specific features encountered, such as three-dimensional effects, the impact of slots as well as trapped modes, which required more efforts to understand and optimise them, are described. In addition, the impedance budget obtained so far is summarised and discussed.

INTRODUCTION

Good knowledge and minimisation of the coupling impedance is of great importance for the future storage ring SOLEIL, envisaged to operate at high current in both multibunch and a few bunch modes. The presence of many transitions due to low-gaps for insertion devices, as well as a relatively small vertical aperture of 25 mm chosen for the standard vacuum chamber, implies appearance of severe transverse collective effects. In view of most chambers not possessing axis-symmetric structures, along with a wide bunch spectrum due to the shorter bunch length, requiring the knowledge of the impedance up to a few tens of GHz, the most reliable approach in evaluating the impedance for our purpose is supposed to use of a 3-dimensional numerical code.

SPECIFIC ASPECTS OF THE STUDIES

Numerical Code Used

Prior to commencing the work, some time was spent in finding the best suited 3D code. Upon comparison, the program GdfidL [1] was chosen, principally for its superiority in performing parallel processed computations with a cluster of processors, gaining a significant factor in terms of speed over mono-processed computations, as well as in its reduced required memory. With GdfidL, the core memory is computer resource limited. As seen below, these two features were critically helpful in treating 3D objects having a fine structure of the order of tenths of millimetres, and in performing long integrations of the wake potential. On the other hand, for a large axis symmetric object such as the SOLEIL cavity, ABCI [2] was used. At SOLEIL, the computer cluster is currently composed of 12 AMD Athlon MP 2000+ at 1.7 GHz, and 4 AMD Opteron at 2.0 GHz, with 20 Gbyte of RAM, running Linux.

Impact of Monopole Fields

The absence of axis symmetry of the vacuum chamber brings about excitation of the wake field even with the passage of the beam on axis. The field is thus monopole in terms of the driving beam, and is known to be quadrupolar in terms of the trailing beam. Namely, a trailing particle is linearly focused transversely. The incoherent tune shift due to the resistive-wall (RW) is evaluated in the complementary paper [3]. The monopole component is disturbing, as it is contained in the usual wakes excited by a dipolar beam. For SOLEIL chambers, they amount to as large as 30~40%. Without the removal of which, the vertical impedance tends to be overestimated and vice versa horizontally. The smallness of the horizontal dipole impedance may even lead to a sign error without correction (i.e. capacitive instead of inductive). The dipole impedance was evaluated by placing the trailing particle on axis in post-processing.

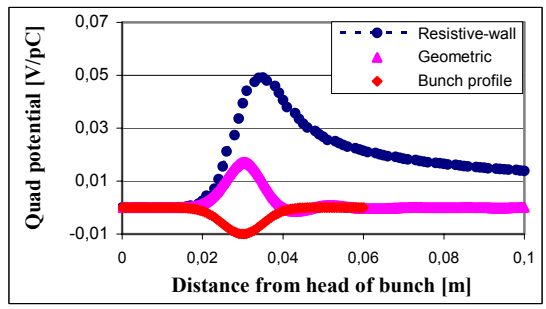

Figure 1: Quadrupole wake in a 5 m long stainless steel chamber with 16 mm vertical gap.

The quadrupolar wake due to the geometric taper impedance was compared with the RW contribution in a typical stainless steel low-gap chamber (Fig. 1). The former was found to be non-negligible, and its relative importance is expected to rise for aluminium chambers.

Dipole Chamber Slot

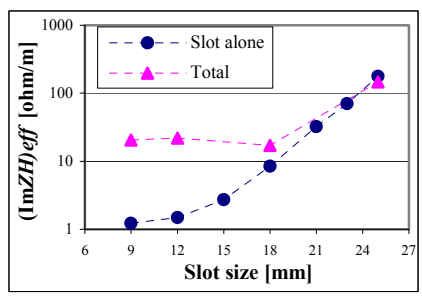

Figure 2: Horizontal impedance versus slot size.

The work was motivated in particular by demands to increase the vertical slot size from its initial value of 9 mm. Numerical results obtained were in agreement with the theory [4] in the following respects: - No dependence of the impedance on slot length. - Steep increase of magnitude with increasing slot opening. - Presence of narrow bands related to the beam pipe cutoffs. By increasing the slot size, the slot impedance exceeded the remaining contributions at around 18 mm slot size (an example shown in Fig. 2). The slot affects predominantly the horizontal impedance, the magnitude of which is

however sufficiently small compared to contributions of other machine components. The latter was also confirmed to be in agreement with studies made elsewhere.

Flanges

The model having a slit of 0.4 mm long and 50 mm deep with no shielding was initially considered. The impedance calculated exhibited strongly trapped modes in all planes from low frequencies, on top of large broadband (BB) impedance (Fig. 3). As the former caused unacceptably low multibunch instability thresholds, a detailed study was launched. Wake potentials were integrated over a long distance (~6 m) to assure good convergence of R/Q's of the trapped modes. Since Q's are infinite in wake computations, eigenvalue computations were carried out to verify the possible overestimation of the effect. By identifying the modes, the surface energy loss due to the resistivity of stainless steel was taken into account to compute the more realistic finite Q values. Shunt impedance R's were then rescaled according to R/Q's previously found. The latter, however, did not much alter the low instability thresholds obtained earlier.

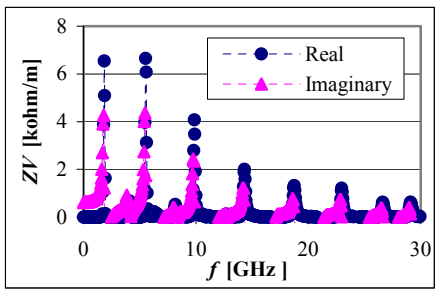

Figure 3: Vertical impedance of the initial flange model.

Both the frequency and amplitude of the narrow bands turned out to depend much on the slit depth, especially at small values. Introduction of short circuiting, as shown in Fig. 4, then led to a dramatic reduction of both the narrow and broadband impedance [5].

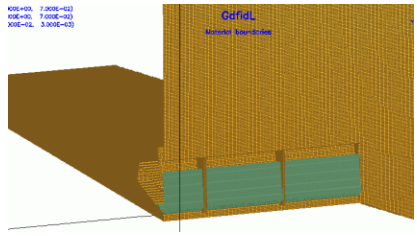

Figure 4: Short circuited flange. The metallic sheet (green) inserted between the two plates effectively shields the cavity-like structure.

BPMs

The sensitivity of the impedance to the gap and thickness of an electrode was investigated in detail, finding an opposing effect between a narrower gap that lowers the impedance and a thinner thickness. The gap was fixed to 0.25 mm [6]. Computations were performed in both the wave guide and short circuited boundary conditions. GdfidL was also used to optimise the electrode transmission line.

Surface Roughness

The work was initiated within the frame of clarifying the impact of NEG coating on the impedance. Besides the two metallic layer model attempted [3], which only qualitatively explains the anomalous impedance increase observed in Elettra [7], the surface roughness is suspected. Attempts are made with GdfidL to characterise the impedance, with reference to analytical approaches.

IMPEDANCE BUDGET

Table 1 summarises the contribution of the machine components evaluated so far in all three planes. Besides the loss factor and the beam power loss at 500 mA in multibunch, the effective impedances are listed, convoluted with the spectrum of a 6 mm long bunch. Real parts of the transverse impedance are evaluated by shifting the bunch spectrum with the chromaticity

Table 1: Impedance budget for SOLEIL obtained so far.

Object	Number	Loss factor	$(P)_{500\ mA}$	$\Sigma\ \lvert Z_L/n\rvert_{eff}$	$(Z_V)_{eff}$	$\Sigma\ \beta_V \times (Z_V)_{eff}$	$(Z_H)_{eff}$	$\Sigma\ \beta_H \times (Z_H)_{eff}$
		[V/pC]	[kW]	[mΩ]	[kΩ/m]	[kΩ]	[kΩ/m]	[kΩ]
Shielded bellows	176	8.72×10^{-3}	**1.17**	**48.30**	(0.03, 0.14)	**(52.8, 246.4)**	(0.01, 0.06)	**(15.8, 112.6)**
Flange[1]	332	4.67×10^{-4}	0.12	11.65	(0.00, 0.01)	(0.7, 42.3)	(0.00, 0.01)	(9.1, 46.8)
Dipole chamber	32	1.64×10^{-4}	2.63×10^{-3}	0.48	(0.00, 0.00)	(0.2, 0.7)	(0.00, 0.03)	(0.1, 0.8)
Soleil cavity	1	2.20	**1.55**	9.30	(0.29, 0.44)	(0.8, 1.3)	(0.17, 0.44)	(0.8, 2.0)
BPM	120	6.10×10^{-3}	0.56	**19.20**	(0.03, 0.05)	(28.8, 54.3)	(0.01, 0.05)	**(21.9, 66.6)**
Medium section tapers	10	1.76×10^{-3}	1.24×10^{-2}	9.31	(1.35, 3.41)	**(85.5, 215.9)**	(0.01, 0.56)	(0.4, 33.7)
Long section tapers	3	7.32×10^{-4}	1.55×10^{-3}	1.52	(0.43, 1.13)	(14.9, 39.2)	(0.00, 0.24)	(0.1, 9.2)
In-vacuum ID tapers[2]	4	0.25	0.76	18.92	(0.50, 1.42)	(6.0, 17.0)	(0.13, 0.50)	(9.4, 36.0)
Soleil cavity outer tapers	1	0.17	0.13	6.70	(0.49, 1.56)	(2.6, 8.3)	(0.01, 0.29)	(0.0, 1.6)
Resistive-wall	-	7.31	**5.17**	**85.50**	(21.8, 101.5)	**(135.2, 743.5)**	(7.10, 51.7)	**(34.8, 376.3)**
Injection zone[2]	1	1.86×10^{-3}	1.42×10^{-3}	0.09	(0.00, 0.01)	(0.0, 0.1)	(0.10, 0.72)	(1.2, 8.7)
Pumping holes (@quads)	128	$< 1.0\times10^{-7}$	$< 1.0\times10^{-7}$	0.01	(0.00, 0.00)	(0.0, 0.0)	(0.00, 0.00)	(0.0, 0.5)
Total	-	-	**9.48**	**211.0**	-	**(327.5, 1369.0)**	-	**(93.6, 694.8)**

1 : The shielded flange as described in the main text
2: At nominal positions

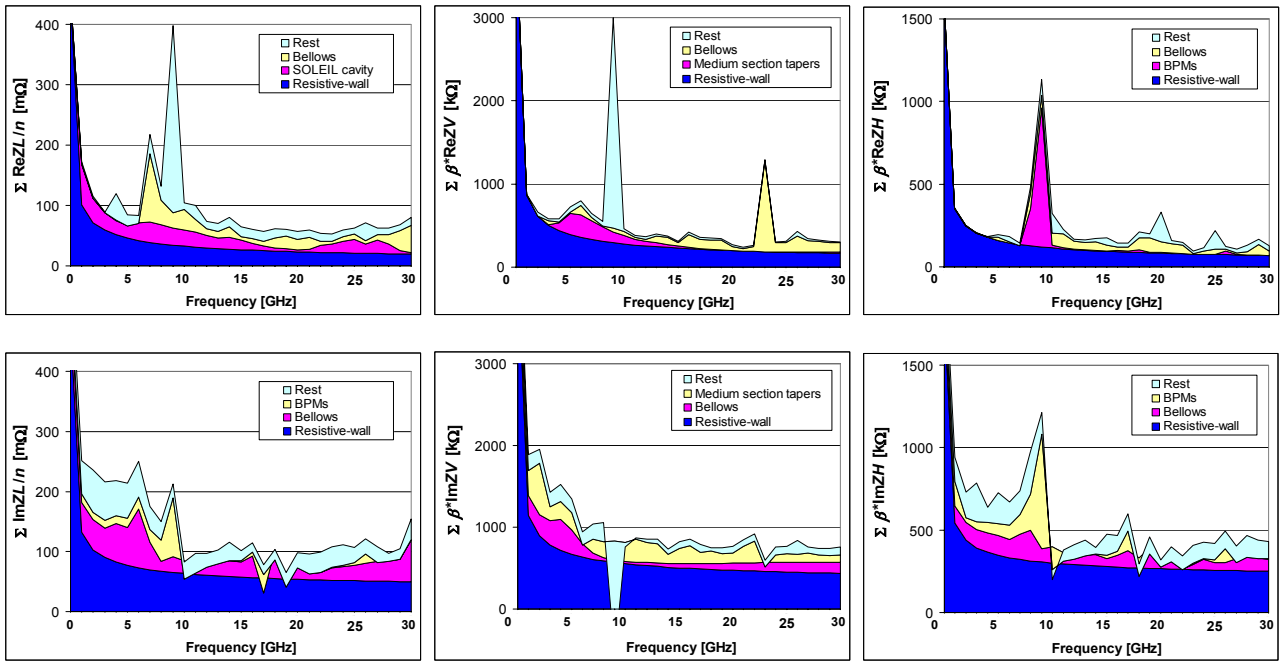

Figures 5: Frequency content of the total impedance in all planes. The three largest contributors are distinguished. Upper: Real part. Lower: Imaginary part. Left: Longitudinal. Centre: Vertical. Right: Horizontal.

(normalised value of 0.3 vertically and 0.1 horizontally), since they vanish otherwise. Also listed in the transverse planes are the sum of the product of the local beta values and the impedance, the quantity that counts for collective effects. Figures 5 display the frequency content of the impedance.

We confirm first of all the domination of the resistive-wall for SOLEIL, which accounts for nearly half or more of the total. Its imaginary part is further enhanced by almost a factor of two due to the NEG layer [3]. Other main contributors found are bellows, BPMs, SOLEIL cavity and tapers (medium straight section). A large peak appearing at around 10 GHz (Figs. 5) comes from BPMs. The impedance is found mostly inductive in all three planes. The horizontal impedance is roughly half of the vertical, which is even larger than the linear ratio of the two apertures (~0.3). Components still to be evaluated include diagnostic elements such as stripline, current transformer, scraper, kickers, and special absorbers. The principal feature of the impedance obtained here is however expected to be unchanged.

CONCLUSION

Thanks to the combination of GdfidL that performs parallel computations and the cluster of processors developed at SOLEIL, most of the heavily 3D objects in SOLEIL were treated with the mesh size of merely few tenths of millimetres and wakes integrated over meters within reasonable times. Among others, $|Z_{//}/n|_{eff}$ for SOLEIL turned out to be around 0.2 Ω, of which roughly half came from the resistive-wall. On the basis of the obtained impedance budget, collective effects are to be studied.

ACKNOWLEDGEMENT

R.N. thanks W. Bruns, the author of GdfidL, for his constant online help and numerous discussions on related subjects, as well as P. Martinez and the computing division of SOLEIL, for the realisation of parallel-processed calculations. Without the two, the achievement of the present results would not have been possible. Thanks are also to T. Günzel (ESRF) for the collaboration on the code comparison and monopole fields, and to C. Herbeaux and other colleagues of the vacuum group for the detailed information on vacuum chambers. The constant support of M.P. Level is to be gratefully acknowledged. Thanks are finally to P. Marchand, J.C. Denard and J.M. Filhol for helpful discussions on the numerical results.

REFERENCES

[1] W. Bruns, "The GdfidL Electromagnetic Field Simulator", http://www.gdfidl.de.
[2] Y.H. Chin, "User's Guide for ABCI Version 8.7", CERN, SL/94-02 (AP).
[3] R. Nagaoka, "Study of Resistive-Wall Effects on SOLEIL", this conference.
[4] G. Stupakov, "Coupling Impedance of a Long Slot and an Array of Slots in a Circular Vacuum Chamber", Phys. Rev. E **51**, 3515 (1995).
[5] C. Herbeaux, private communication, SOLEIL.
[6] J.C. Denard, private communication, SOLEIL.
[7] E. Karantzoulis et al., "Broad band Impedance Measurements on the Electron Storage Ring ELETTRA", Phys. Rev. ST-AB **6**, 030703 (2003).